Dynamics of an octahedral Cu2+ jahn-teller system. consequences on its electron spin resonance

Le Si Dang, R. Buisson, F.I.B. Williams

Classification
Physics Abstracts
0.660 — 0.665

DYNAMICS OF AN OCTAHEDRAL Cu^{2+} JAHN-TELLER SYSTEM. CONSEQUENCES ON ITS ELECTRON SPIN RESONANCE

LE SI DANG and R. BUISSON

Laboratoire de Spectrométrie Physique,
Université Scientifique et Médicale de Grenoble, France

and

F. I. B. WILLIAMS

Service de Physique du Solide et de Résonance Magnétique, Orme des Merisiers,
Commissariat à l'Energie Atomique, BP 2, 91190 Gif-sur-Yvette, France

(*Reçu le 5 juillet 1973*)

Résumé. — La déformation du complexe $Cu^{2+}(OH_2)_6$ résultant de l'effet Jahn-Teller et le saut d'une déformation à une autre sont étudiés expérimentalement à partir de plusieurs de leurs conséquences : temps de relaxation spin-réseau, élargissement des raies de résonance, modification du spectre RPE en fonction de la température. La vitesse de saut d'une déformation à l'autre déduite des mesures de l'élargissement des raies et le temps de relaxation spin-réseau varient tous les deux avec la température selon une loi en T^3. L'évolution du spectre RPE avec la température est étudiée attentivement pour plusieurs orientations du champ magnétique jusqu'à disparition du spectre anisotrope et apparition du spectre isotrope. Les résultats des mesures du temps de relaxation et de la vitesse de saut s'expliquent bien à partir d'un travail précédent. Une théorie des conséquences sur le spectre RPE des sauts est faite à l'aide d'une théorie stochastique. Après une description de l'évolution du spectre d'un système simple, le cas plus compliqué du système $Cu^{2+}(OH_2)_6$ est traité et les résultats de cette théorie permettent d'expliquer les observations expérimentales de façon très satisfaisante.

Abstract. — The $Cu^{2+}(H_2O)_6$ complex in zinc fluosilicate is subject to a « static » Jahn-Teller effect. It is well known that its spin resonance spectrum changes from one of tetragonal symmetry at low temperatures to become isotropic at high temperatures. We have made a detailed experimental study of this transition between 1.2 K and 80 K and compared the observations with the spectral features worked out from a model where the crystal vibrations cause the complex to reorient between the three strain stabilised tetragonal distortions. The model accounts very well for the observations without having to invoke excited levels. The reorientation rate $1/\tau \approx 1.2 \times 10^5\ T^3\ s^{-1}$ was deduced from line broadening for $4.2 < T < 18$ K and its extrapolation to higher temperatures confirmed by comparison with theoretically reconstructed spectra for H along $< 100 >$ and $< 111 >$ directions. The spin lattice relaxation time $1/T_1 \approx 800\ T^3\ s^{-1}$ for $1.2 < T < 4.2$ K. The « isotropic » spectrum shows a small trigonal anisotropy from which we estimate the parameters describing the trigonal component of the crystal field and calculate their effect in the low temperature region.

1. **Introduction.** — Since the original proposition of Jahn and Teller [1], much work has been devoted to finding systems which show that the predicted effect exists and to explaining more and more details of the observations. The work of Ham and O'Brien, following the pionneer ideas of Abragam and Pryce [2], have largely clarified the situation for the spectroscopic properties of Jahn-Teller ions [3]. Over the last few years the problem of the dynamics of these systems has begun to be studied quantitatively.

By way of illustration and introduction to the present paper, we would cite the work of Williams, Krupka and Breen [4], [5] (these papers are referred here as I and II) who, by measuring the relaxation times T_1 and the reorientation times τ of divalent copper in double nitrate, demonstrated the influence of the dynamics of the J.-T. effect on the relaxation : T_1 was 10^4 shorter than in similar compounds where J.-T. effect is not present. The theory of this enhancement of the relaxation rate was given in II and explains the experiments relatively well. In this paper, we give the results we have obtained with divalent copper in the fluosilicate. They are again in good and in some respects better agreement with the theory. We have also studied quantitatively the change of the spectrum with the temperature, an aspect of the J.-T.

effect pointed out from the very first observation of Bleaney and Ingram [6] but which has never been studied in detail. We report here our experimental observations and we give a theoretical explanation within the model developed in II.

The first part of this work gives the experimental results for the relaxation time T_1, the reorientation time τ and the averaging of the spectrum. In the second part we present the theory of this averaging and in the last part, we compare the theoretical predictions with the experiments and make some remarks on the values of T_1 and τ in view of the predictions of II.

2. **Experimental results.** — Zinc fluosilicate ($ZnSiF_6$, 6 H_2O) is of CsCl type structure, the Cs and Cl ions being replaced by SiF_6 and $Zn(H_2O)_6$ octahedra [7]. Cu^{2+} enters the crystal in substitution for Zn^{2+}, and thus is submitted to an octahedral crystal field. However, due to the next nearest neighbours, the symmetry is slightly trigonal. For our experiments, we have used two deuterated samples. A chemical analysis on a third sample grown from the same solution has shown that the concentration is 0.2 % Cu^{2+} ions with respect to Zn^{2+} ions.

2.1 EPR SPECTRUM. — The EPR of divalent copper in zinc fluosilicate was observed many years ago by Bleaney *et al.* [6], [8]. At liquid helium temperature, one observes three spectra of axial symmetry, each corresponding to an octahedron distorted along one of the three fourfold axes by the Jahn-Teller effect. Figure 1 shows the observed spectra for the magnetic field H along the $< 100 >$ and $< 111 >$ directions. For the former, the low field group of lines corresponds to the « parallel » centers and the high field group to the « perpendicular » centers. For the latter, all the centers are equivalent. We find the following spin Hamiltonian parameters :

$$g_{\parallel} = 2.460 \pm 0.005$$

$$g_{\perp} = 2.100 \pm 0.005$$

$$|A_{\parallel}| = (107 \pm 2) \times 10^{-4}\ \mathrm{cm}^{-1}$$

$$|A_{\perp}| = (14 \pm 2) \times 10^{-4}\ \mathrm{cm}^{-1}$$

$$A_{\parallel} \times A_{\perp} < 0$$

($S = \frac{1}{2}$, $I = \frac{3}{2}$). The values of the hyperfine constants are an average due to the presence of the two isotopes Cu^{63} and Cu^{65} with respective natural abundance 69 % and 31 %. The labelling of the hyperfine lines is made on the assumption $A_{\parallel} < 0$, as found in double nitrate [4]. The value of $A_{\perp}$ given here is deduced from the averaged (high temperature) hyperfine parameters as explained in paragraph 4.1.

At liquid nitrogen temperature, one observes a single axial spectrum (Fig. 2 and 3) whose axis of symmetry is $< 111 >$ and whose Hamiltonian parameters are now :

$$g'_{\parallel} = 2.22 \pm 0.01$$

$$g'_{\perp} = 2.23 \pm 0.01$$

$$g'_{\perp} - g'_{\parallel} = 0.010 \pm 0.001$$

$$|A'_{\parallel}| = (21 \pm 2) \times 10^{-4}\ \mathrm{cm}^{-1}$$

$$|A'_{\perp}| = (29 \pm 2) \times 10^{-4}\ \mathrm{cm}^{-1}.$$

All these values are in accord with those of Bleaney, Bowers and Trenam [8].

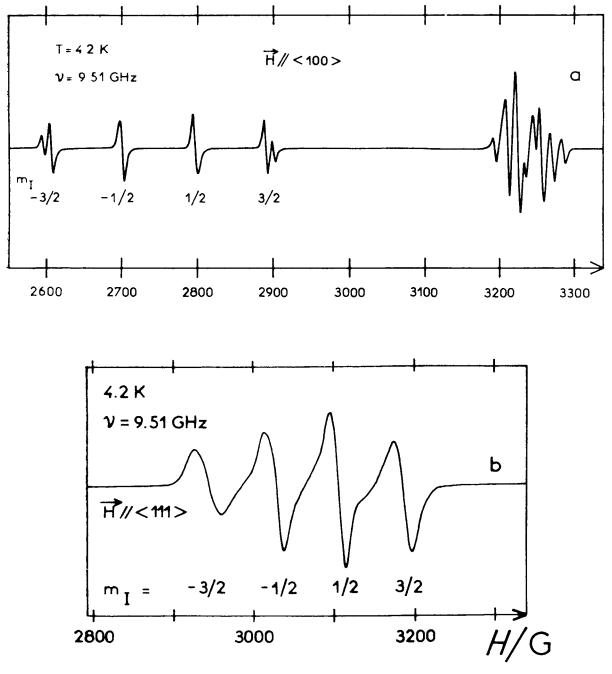

FIG. 1. — EPR spectrum observed at $T = 4.2$ K with a resonance frequency of 9 510 MHz : *a*) with the magnetic field along a $< 100 >$ direction ; *b*) with the magnetic field along a $< 111 >$ direction.

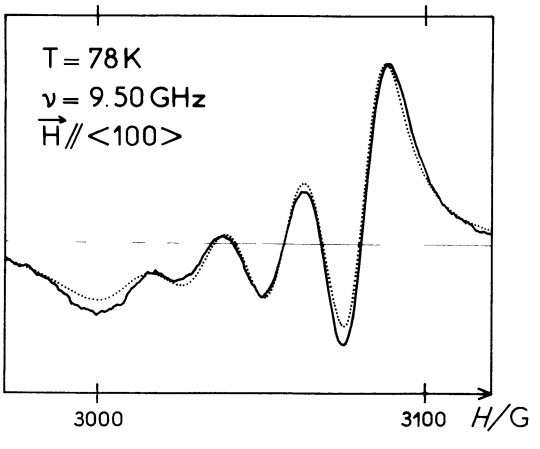

FIG. 2. — Solid line : EPR spectrum observed at $T = 78$ K with the magnetic field along a $< 100 >$ direction.
Dotted line : Calculated spectrum as indicated in section 4.1 with the values $\omega_e = 1.5 \times 10^{10}\ \mathrm{s}^{-1}$ and $1/T_1 = 2.4 \times 10^{7}\ \mathrm{s}^{-1}$.

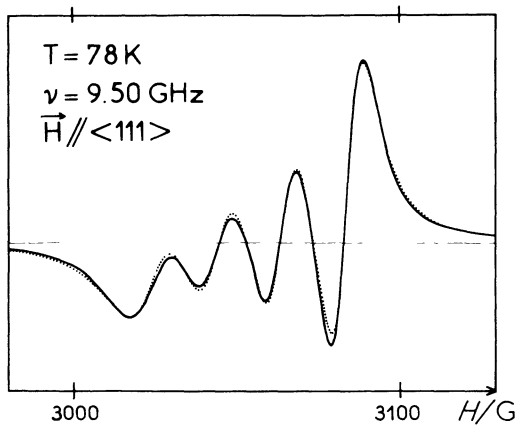

FIG. 3. — Solid line : EPR spectrum observed at $T = 78$ K with the magnetic field along a $< 111 >$ direction.
Dotted line : Calculated spectrum as indicated in section 4.2 with the values $\omega_e = 9 \times 10^9\ s^{-1}$ and $1/T_1 = 2.1 \times 10^7\ s^{-1}$.

2.2 RELAXATION TIME MEASUREMENTS [9]. — The relaxation time T_1 was measured with an apparatus described elsewhere [10], using the standard method of saturating the EPR transition with a high power pulse and monitoring the recovery signal. The length of the pulse was about 15 μs. After the saturating pulse, a fast variation of the signal was observed, followed by an exponential decay. We have considered only this part, the fast variation being due possibly to spin diffusion [4].

With the magnetic field H along the $< 100 >$ direction, and in the temperature range 1.2-4.2 K, we find the following :

(i) Within our experimental accuracy (10 % for time measurements and 0.1 K for temperature measurements), T_1 does not vary significantly from line to line belonging to the same group.

(ii) T_1 is shorter for the « perpendicular » group than for the « parallel » group, the difference being about 30 %.

(iii) For $m_I = -\frac{3}{2}$ and $m_I = -\frac{1}{2}$ hyperfine lines of the « parallel » group, the results shown on figure 4*a* are well fitted by :

$$\frac{1}{T_1} = (800 \pm 100) \times T^3\ (s^{-1}) \quad (1.2\ K < T_\perp < 4.2\ K)\ .$$

We have also measured the anisotropy of T_1 for these lines :

$$\frac{T_1[111]}{T_1[100]} = 0.6 \pm 0.1 \qquad (1.2\ K < T < 4.2\ K)$$

$$\frac{T_1[110]}{T_1[100]} = 0.8 \pm 0.1 \qquad (1.2\ K < T < 4.2\ K)\ .$$

2.3 LINEWIDTH MEASUREMENTS [9]. — As shown in reference [5], the interwell tunneling induces a loss of phase for the spin precession, and accordingly a broadening of the resonance line. At low temperatures, where the effect is negligible, the static line shape is very well approximated by a Gaussian. We suppose (see discussion in § 3) that the effect of the tunneling

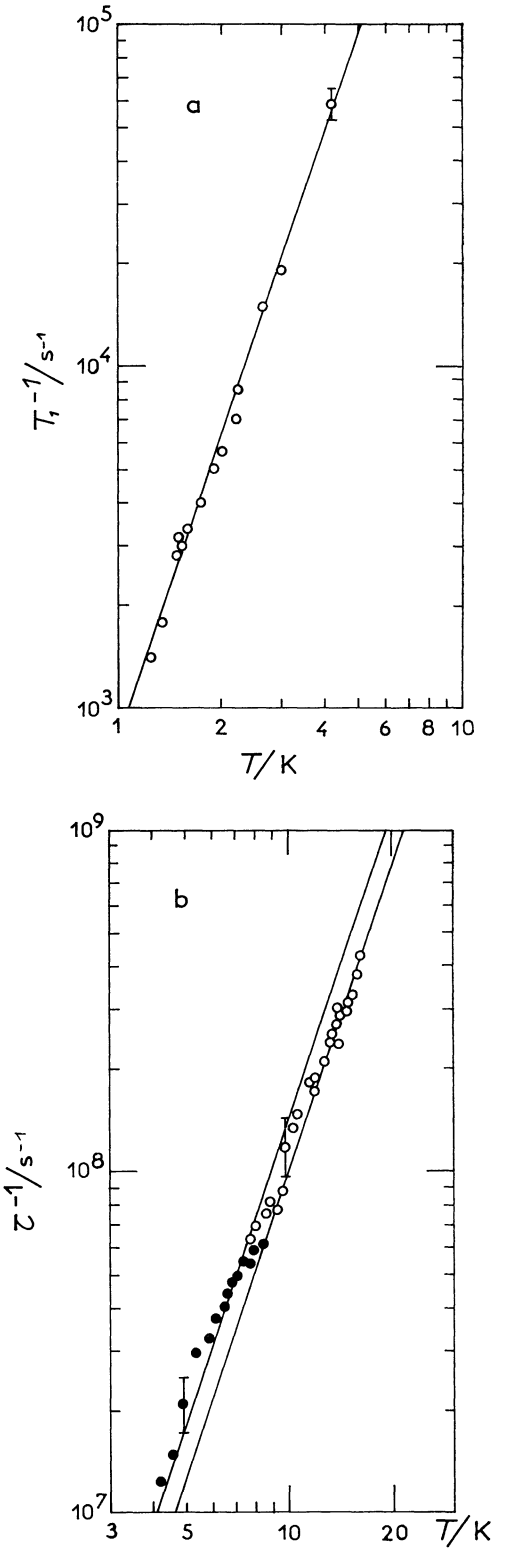

FIG. 4. — *a*) Averaged values of the relaxation times measured on the $m_I = -\frac{3}{2}$ and $m_I = \frac{1}{2}$ lines of the low field group with H along a $< 100 >$ direction.
b) Reorientation time deduced from the linewidth measurements on the $m_I = \frac{3}{2}$ line (●) and on the $m_I = -\frac{1}{2}$ line (○) with the magnetic field along a $< 100 >$ direction.

on the line shape may be calculated by convoluting the Lorentzian

$$L(\omega - \omega_0) = \frac{1}{\pi} \cdot \frac{\sqrt{3}\,\Delta_L}{(\omega - \omega_0)^2 + 3\,\Delta_L^2}$$

where Δ_L is the half peak to peak width related to the more usual T_2 by $1/T_2 = \sqrt{3}\,\Delta_L$, with the static Gaussian to give, for the observed derivative of absorption

$$F(x, k) = -\frac{k}{\pi\sqrt{\pi}} \cdot \frac{\sqrt{2}}{\Delta_G} \int_{-\infty}^{+\infty} \frac{(x - y)\,e^{-y^2}\,dy}{[(x - y)^2 + k^2]^2} \qquad (1)$$

where Δ_G is the half peak to peak width of the Gaussian,

$$k = \sqrt{\frac{3}{2}} \cdot \frac{\Delta_L}{\Delta_G}, \qquad x = \frac{1}{\sqrt{2}} \cdot \frac{\omega - \omega_0}{\Delta_G}$$

(the ω's are related to magnetic field values by

$$\omega = \frac{g\beta}{\hbar} H\Big).$$

The curve shown on figure 5 represents the half peak to peak width Δ of the resulting line $F(x, k)$ as a function of Δ_L, for $\Delta_G = 1$. So by measuring Δ_G at 1.2 K and Δ, we can deduce Δ_L and so T_2.

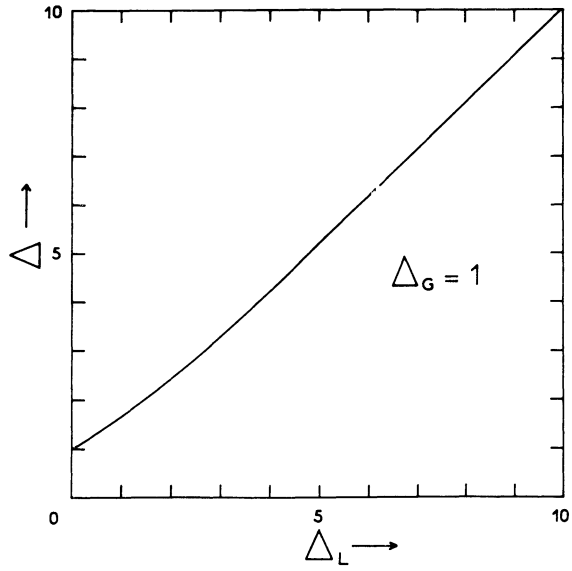

FIG. 5. — Value of the half peak to peak width of the line resulting from the convolution of a Gaussian of half peak to peak $\Delta_G = 1$ with a Lorentzian of half peak to peak width Δ_L obtained from eq. (1).

Our measurements are made on the « parallel » group of lines with the magnetic field along the $< 100 >$ direction when $1/T_2$ is identical to the tunneling rate ω_c (see section 3.2). In the temperature range 4.2-8 K, the isotopic splitting of the $m_I = \pm \frac{3}{2}$ hyperfine lines is well resolved and it is easy to measure their separate broadening (see Fig. 1). For 8-18 K, the linewidths are much larger than the isotopic splitting of the $m_I = \pm \frac{1}{2}$ hyperfine lines and it is more convenient to measure these. The experimental results are given on figure 4*b*, and are well fitted by :

$$\omega_c = \frac{1}{\tau} = (1.25 \pm 0.25) \times 10^5 \times T^3\,(s^{-1})$$

$$4.2\ K < T < 18\ K\,.$$

Although T_1 and τ are not measured in the same temperature range, we have observed the same T^3 dependence, and by extrapolation we deduce that :

$$R = \frac{1/T_1}{1/\tau} = 6.4 \times 10^{-3}$$

for H along a $< 100 >$ direction.

2.4 MODIFICATION OF THE SPECTRUM WITH THE TEMPERATURE. — We have studied the evolution of the tetragonal spectra as a function of the temperature. Figures 6 and 7 show this evolution for H

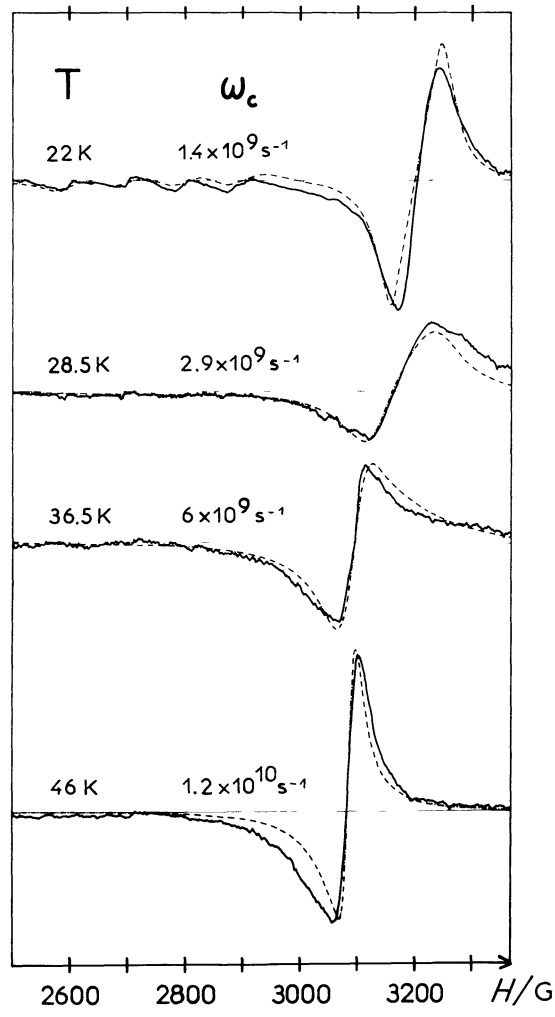

FIG. 6. — Evolution of the EPR spectrum with the temperature when the magnetic field is along a $< 100 >$ direction :
Solid lines : experimental spectrum.
Dotted lines : calculated spectrum from eq. (5) with the values of ω_c deduced from the T^3 law.

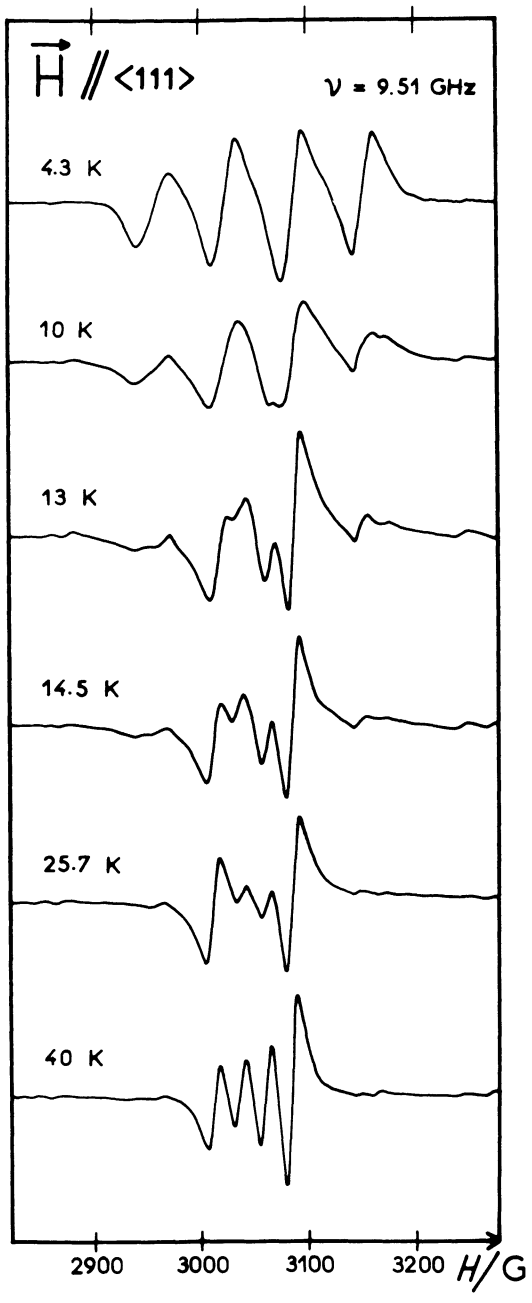

FIG. 7. — Evolution of the EPR spectrum with the temperature when the magnetic field is along a < 111 > direction.

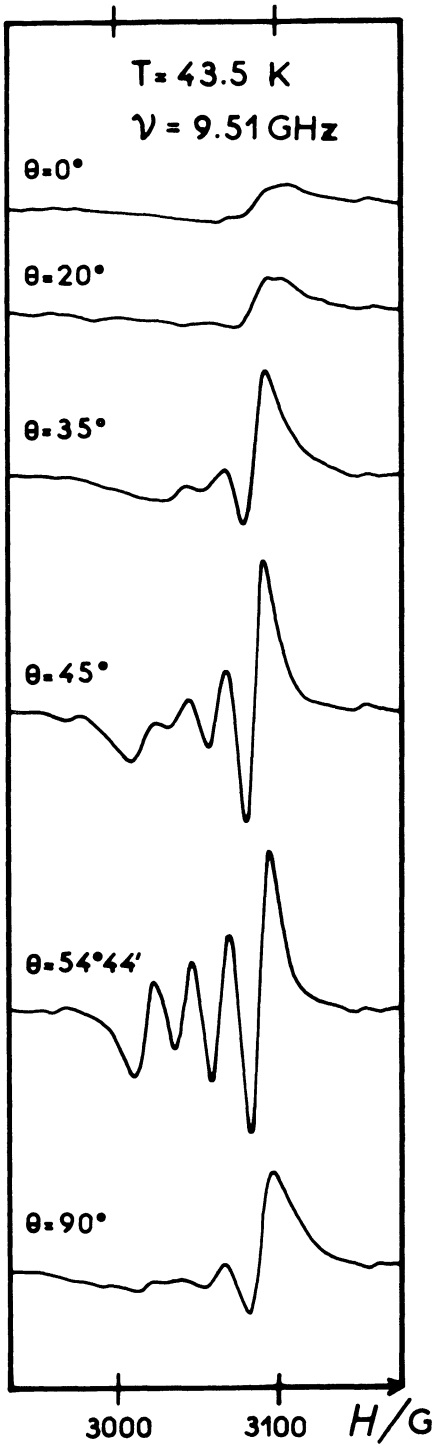

FIG. 8. — Evolution of the EPR spectrum with the magnetic field orientation at $T = 43.5$ K. The magnetic field lies in the (110) plane and makes the angle θ with the [001] axis.

along a < 100 > and < 111 > direction, while figure 8 shows the modification of the spectrum when H rotates in a { 110 } plane at a fixed temperature $T = 43.5$ K.

From these spectra, we see that the « transition temperature » is strongly dependent on the magnetic field orientation : it is about 40 K for H parallel to < 100 > and about 13 K for H parallel to < 111 >. We have noted below the general features of these spectra.

2.4.1 *H along* < 100 > (Fig. 6). — (i) The « perpendicular » group, which results from a great number of overlapping lines, is visible at higher temperatures than the « parallel » group. It shifts towards low magnetic field when the temperature increases.

(ii) For $T > 40$ K, the width of the unique line decreases as the temperature increases. In the nitrogen temperature range, the spectrum takes the well known shape consisting of four hyperfine lines of unequal widths (see Fig. 2), and broadens again beyond.

(iii) For $T > 120$ K, the broadened spectrum progressively disappears.

2.4.2 *H along* $< 111 >$ (Fig. 7). — (i) Up to 8 K, we observe only the low temperature spectrum. Its hyperfine lines have nearly equal and constant width.

(ii) For higher temperatures, the intensity of the low temperature spectrum decreases, while another spectrum progressively appears with an hyperfine structure constant equal to about a third of the preceding. These two spectra are both present in the range 8-27 K.

We describe now the evolution of the new spectrum.

(iii) At any temperature, the $m_I = + \frac{3}{2}$ line is always the narrowest.

(iv) Between 13 K and 27 K, the $m_I = \pm \frac{3}{2}$ lines are narrower than the $m_I = \pm \frac{1}{2}$ lines.

(v) At 40 K, the $m_I = - \frac{3}{2}$ and $m_I = \pm \frac{1}{2}$ lines have approximately the same width. For higher temperatures, the spectrum changes progressively to become similar to the high temperature $< 100 >$ spectrum but with narrower lines.

Most of these experimental observations will be explained by a theory of the averaging given in the next section.

2.5 COMPARISON WITH OTHER EXPERIMENTS. — Relaxation time and reorientation time measurements have been made by Breen, Krupka and Williams [4] and by Lee and Walsh [11] on the two similar systems : Cu^{2+} in magnesium Lanthanum double nitrate and zinc bromate. The results are significantly different from those reported here since the temperature dependence of these times was observed to be of the form $\alpha T + \beta T^5$ (for $1.3 < T < 10$ K) for the double nitrate and αT ($1.3 < T < 10$ K) for the bromate [4]. They have however two common points with ours, namely : a similar weak anisotropy for T_1 and nearly equal values for the ratio τ/T_1 (2×10^{-3} in double nitrate and 6.4×10^{-3} here).

The change of the EPR spectrum with the temperature was not studied in detail for these two systems where only the broadening of the lines was pointed out for the isotropic spectrum with $T > 130$ K. However, evolutions similar to that reported here have very often been observed. The review paper of Ham on Jahn-Teller effect [3] gives a voluminous bibliography in which one can find references to these works which concern either systems equivalent to ours like Cu^{2+} in NaCl by Borcherts *et al.* [12], Cu^{2+} in $Ca(OH)_2$ by Wilson *et al.* [13] or different systems like Fluorine in BeO by Reinberg and Estle [14], phosphorous vacancy pair in silicon by Watkins and Corbett [15]. In most of these works, an exponential dependence of the reorientation time was observed which shows that the mechanisms can be different to those considered here. In the work of Borcherts *et al.* [12], the coexistence at 95 K of the low temperature anisotropic spectrum with an isotropic spectrum was pointed out and the later was attributed to the resonance in an excited vibronic level. Wilson *et al.* [13] have also reported an averaging of the low temperature spectrum ; their observations are very similar to ours but there are differences in the interpretation.

3. **Theory.** — There are three parts to this section. The first (3.1) contains a description of the evolution of the spin resonance spectrum of a very simple 2-well model with relaxation in order to illustrate as clearly as possible the physical ideas without the encombering details which are necessary for describing our real system, a task we undertake in the second part (3.2). In the third part (3.3) we carry the analysis of the effects of a trigonal crystal field a little further than was done in II, in particular the effects on the hyperfine structure ; a certain number of calculational errors of II are also corrected.

The calculation of the spectral evolution is an exercise in applying the ideas and techniques of Anderson [16], Anderson and Weiss [17] and Kubo [18]. We shall see that it is even a good pedagogical demonstration of « motional averaging » where one can control both the rapidity of the fluctuations and the form of the modulated hamiltonian. However we shall only calculate in detail the cases of H_0 along [100] and [111] directions.

3.1 A DOUBLE-WELL $S = \frac{1}{2}$ SYSTEM WITH RELAXATION. — Imagine a system-initially without spin — which moves with some effective mass in the double well potential of figure 9 of hump height $h \gg \hbar\omega_0$

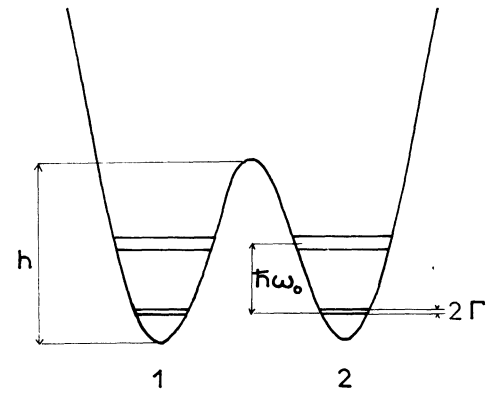

FIG. 9. — Double well potential used in the model studied in section 3.1.

where ω_0 is the resonance frequency for small displacements in a well. The doubly degenerate ground state appropriate to an infinitely high barrier is spanned by states ψ_1 and ψ_2 localized in wells 1 and 2 respectively. On lowering the barrier, these states become less localized and interact to break the degeneracy by a « tunneling » energy 2Γ ; the eigenstates are evidently symmetric and antisymmetric under well

interchange and are to a good approximation $\psi_s = \sqrt{\frac{1}{2}}(\psi_1 \pm \psi_2)$. Consider now the effect of an external perturbation. It may always be divided into a sum of two parts — one symmetric and the other antisymmetric with respect to the two wells. Only the latter, which distinguishes between wells, will tend to localise the system ; e. g. if the two wells are rendered inequivalent in energy by $\Delta \gg \Gamma$, the new eigenstates are $\psi_1 \pm (\Gamma/\Delta)\psi_2$, i. e. the eigenstates are essentially localised in each well ; we can say that the asymmetric perturbation has « quenched » the tunneling.

A word on « tunneling » in our context. The « quantum mechanical tunneling frequency » $2\,\Gamma/\hbar$ is the oscillation rate between wells *in the absence of an external perturbation* if the system has been prepared localised in a single well and then left to evolve freely. An observation can tell us in which well a system is only if it is associated with an antisymmetric perturbation which localizes the states, the spatial part of the eigenfunction being then approximately ψ_1 or ψ_2 with corresponding value ε_1 or ε_2, say, for the observable. We shall call this perturbation an « observing perturbation » even if in real systems it does not depend on the experimentalist as it is the case for random strains in crystals. If the system is otherwise isolated, it will remain in the eigenstate corresponding to the reading (ε_1, say) until the observing perturbation is removed, from which moment ($t = 0$, say) we must solve the unperturbed equation of motion subject to the initial condition $\psi\ (t = 0) = \psi_1$. Then

$$\psi(t) = \cos\frac{\Gamma}{\hbar}t\psi_1 + \mathrm{i}\sin\frac{\Gamma}{\hbar}t\psi_2$$

and if we do the same experiment at time τ, we have probabilities $\cos^2 \Gamma\tau/\hbar$ and $\sin^2 \Gamma\tau/\hbar$ of finding results ε_1 and ε_2 respectively, i. e. the site localisation probability oscillates with period $h/2\,\Gamma$ if it is free of external (including the observing), perturbations. On the other hand, had we left on the observing perturbation, the otherwise isolated system would have stayed in the well in which it was found, for that condition is an eigenstate and remains so.

However if our system is coupled to another (e. g. the phonons) to whose state our measurement is insensitive, energy may be exchanged between the two inducing a transition from ψ_1 to ψ_2 and so changing the experimental reading from ε_1 to ε_2 (the phonon system changes state simultaneously, but we are not looking at that).

We stress that our experiment corresponds to the latter, for we leave on permanently the perturbation of the observation (magnetic field or local strain). We do not see directly the quantum mechanical tunnelling, but only the phonon induced transitions — often called « phonon assisted tunnelling » when only the ground states are involved, for it requires both the tunnelling matrix element Γ and the phonon interaction since the latter does not directly connect ψ_1 to ψ_2. In particular, there is no « zero-temperature tunnelling » and a low temperature temperature-independent transition rate does not give Γ directly, but the spontaneous decay rate by phonon creation from an excited well state.

We return now to our model system to see how the spin resonance might be used as an observable for the spatial configuration and what are the effects on this EPR spectrum of the coupling with the lattice vibrations.

Suppose then that our model system has a Kramers degeneracy, for which we introduce a fictitions spin $S = \frac{1}{2}$. To fix ideas, let well 1 correspond to a distortion with symmetry around the z-axis and well 2 to a distortion with symmetry around the x-axis. This might occasion an anisotropy of the g-tensor through the orbital magnetic moment. We suppose the principal directions for the g-tensors in each case to lie along (xyz) axes, but the principal values to be interchanged for the two wells, i. e. $\underline{g}_1 = (g_\parallel, g_\perp)$, $\underline{g}_2 = (g_\perp, g_\parallel)$ where we have only written the z and x principal values for simplicity as we shall confine **H** to be in the zx plane. In such a situation we can use the EPR spectrum to observe the spatial configuration.

If **H** makes angle θ with the z-axis, we may write the magnetic interaction

$$\mathcal{H}^z = \Omega(S_z\cos\theta + S_x\sin\theta) + \\ + b\omega(S_z\cos\theta - S_x\sin\theta) \quad (2)$$

where b is a variable of the spatial configuration whose matrix in the basis ψ_1, ψ_2 is

$$[b] = \begin{bmatrix} +1 & \\ & -1 \end{bmatrix} \quad \text{and} \quad \begin{matrix} \Omega = \frac{1}{2}(g_\parallel + g_\perp)\,\mu_B H \\ \omega = \frac{1}{2}(g_\parallel - g_\perp)\,\mu_B H \end{matrix}.$$

The ω part of this hamiltonian distinguishes between wells ; a pure well 1 state has a resonance line at $g_1^2 = g_\parallel^2\cos^2\theta + g_\perp^2\sin^2\theta$, a pure well 2 state at $g_2^2 = g_\parallel^2\sin^2\theta + g_\perp^2\cos^2\theta$ and mixtures at g_m where $g_1 < g_m < g_2$.

Suppose that the local strains — or even the anisotropic Zeeman interaction — are such as to leave nearly pure well 1 or well 2 states. Experimentally, this could be verified by the presence of the two spin resonance g-factors of g_1 and g_2 at low temperatures when the relaxation is slow. As one raises the temperature the thermal phonons induce relaxation between the two well states, either by a one-phonon phonon-assisted tunnelling process or a multiphonon process, depending on the temperature. We suppose that this relaxation is described by a relaxation time $\tau_c = 1/\omega_c$ which is independent of the energy difference Δ between well states and that $\Delta \ll kT$ so that $W_{1\to 2} \approx W_{2\to 1}$. In these circumstance, we may describe the motion of the magnetic moment by hamiltonian (2) where $b = b(t)$ becomes a stochastic variable which has equal probabilities for its two

values ± 1 and whose fluctuations are described by a stationary Markoff process of jump probability ω_C s^{-1}. The autocorrelation function for b is then

$$\overline{b(t)\, b(t+\tau)} = \exp - \omega_C \mid \tau \mid .$$

The form of the stochastic hamiltonian varies with the magnetic field orientation, but we shall select two particularly simple situations.

(i) $\theta = 0 \quad \mathcal{H}(t) = \big(\Omega + \omega b(t)\big)\, S_z$

the pure adiabatic case and

(ii) $\theta = \dfrac{\pi}{4} \quad \mathcal{H}(t) = \Omega S_Z + \omega b(t)\, S_X ,$

the pure non-adiabatic case, where an obvious change of axes has been made.

The solutions may be found in the literature (Kubo [18], Winter [19], Abragam [20]), but we recall them here for completeness.

Case (i) $\mathcal{H}(t) = \big[\Omega + \omega b(t)\big]\, S_z$.

If $\omega_c \ll \omega$, the situation is static with resonance lines at frequencies $\Omega_i = \Omega \pm \omega$ of widths (transverse relaxation rates) $1/T_2 = \omega_c$. When $\omega_c \gg \omega$, there is a single line at Ω of width ω^2/ω_c (motional narrowing). The problem may be solved exactly and the absorptive susceptibility at (circular) frequency ν is given by

$$X''(\nu) = \text{Cte}\, \frac{(2\,\omega)^2}{(\Omega+\omega-\nu)^2\,(\Omega-\omega-\nu)^2+\omega_c^2(\Omega-\nu)^2} .$$

This « adiabatic » width arises uniquely from the fluctuations in resonant frequency — the spin eigenstates are identical for the two values of $b(t)$ and there is no longitudinal relaxation ($1/T_1 = 0$). The characteristic frequency for « rapidity » is $2\,\omega$, the difference in resonant frequencies for the two « static » lines.

Case (ii) $\mathcal{H} = \Omega S_z + \omega b(t)\, S_x$.

The fluctuating field is purely transverse and the absolute value of the total field is independent of the instantaneous value of b. For $\omega/\Omega \ll 1$, there is a single resonance line centred on

$$\omega_0 = \Omega\left(1 + \frac{1}{2}\,\frac{\omega^2}{\Omega^2 + \omega_c^2}\right)$$

of width

$$\Delta\omega = \frac{1}{T_2} = \frac{1}{2}\,\frac{\omega^2\,\omega_c}{\Omega^2 + \omega_c^2}$$

and of longitudinal relaxation rate

$$\frac{1}{T_1} = \frac{2}{T_2} .$$

In the static limit $\omega_c \ll \Omega$,

$$\omega_0^2 \to \Omega^2 + \omega^2$$

$$\frac{1}{T_2} = \frac{1}{2}\,\frac{1}{T_1} \to \frac{1}{2}\,\omega_c \left(\frac{\omega}{\Omega}\right)^2$$

whereas in the dynamic (« motional narrowing ») limit $\omega_c \gg \Omega$

$$\omega_0 \to \Omega$$

$$\frac{1}{T_2} = \frac{1}{2}\,\frac{1}{T_1} \to \frac{1}{2}\,\frac{\omega^2}{\omega_c} .$$

This « non-adiabatic » width arises from the fact that the eigenstates are not identical for $b = \pm 1$, meaning that « transitions » are induced as b fluctuates. In another language, the component of the fluctuating transverse field at the frequency Ω induces transitions which destroy both the phase and the longitudinal magnetization of the spin.

$1/T_1$ in the slow limit is just the effect of the non-orthogonality of the spin eigenstates for $b = +1$ to those of $b = -1$. The angle between the two quantization axes for $b = \pm 1$ is $\beta \approx 2\,\omega/\Omega$ if $\omega \ll \Omega$ and the projection of $\mid + \tfrac{1}{2}\,; b = +1 >$ onto $\mid - \tfrac{1}{2}\,; b = -1 >$ is $\sin \beta/2 \approx \omega/\Omega$ (the value of b in the ket is to show in what system of axes the value of M_s is to be understood), the square of which, by the reasoning of Williams, Krupka and Breen [5], is to be multiplied by ω_c to find $1/T_1$. It is to be remarked, however, that when $\omega_c \gg \Omega$ and the eigenstates are always very nearly $\mid \pm \tfrac{1}{2}\,; b = 0 >$, $1/T_1 \to 0$. In this limit, $1/T_1$ may be understood by considering the time necessary for the value of the square of the admixture coefficient of the $\mid - \tfrac{1}{2}\,; b = 0 >$ state to become ~ 1, having prepared the system in a pure $\mid + \tfrac{1}{2}\,; b = 0 >$ state at time 0 (the error step in the admixture is $\sim$ i $2\,\Omega(\omega/2\,\Omega)\,(1/\omega_c)$ for $\Omega \ll \omega_c$ and the number of steps in time T_1 is $\sim \omega_c\, T_1$; for the static situation, $\omega_c \ll \Omega$, the error step is $\sim \pm\, \omega/\Omega$, and the same sort of argument may again be used). The characteristic frequency for rapidity in this case is no longer a difference in static resonant frequencies — there is none — but the precession frequency Ω.

3.2 THE THREE WELL $S = \frac{1}{2}$ MODEL — Cu^{2+}/FLUOSILICATE, ETC. — Bearing in mind these simple results we examine our own case. We shall find that if H_0 is along a [100] axis, there is only « adiabatic » broadening and averaging whereas if H_0 is along a [111] axis there is only « non-adiabatic » broadening and averaging. Intermediate orientations offer a mixture of the two.

The spin hamiltonian of a centre depends on the distortion state in which it finds itself. We express this by writing

$$\mathcal{H}(t) = a_1(t)\, \mathcal{H}^x + a_2(t)\, \mathcal{H}^y + a_3(t)\, \mathcal{H}^z , \qquad (3)$$

where $\mathcal{H}^i$ is the spin hamiltonian appropriate to a state with i-distortion ($i = x$, y, or z) and the triad

$$S(t) = \big(a_1(t), a_2(t), a_3(t)\big)$$

takes on the values (100), (010) and (001) for x, y or z-distortions respectively ; $a_1(t) + a_2(t) + a_3(t) = 1$.

To simplify somewhat we limit the spin Hamiltonian

to the Zeeman and magnetic hyperfine interactions in cubic symmetry.

Thus

$$\mathcal{H}^x = \Omega H^{-1}\,\mathbf{H}.\mathbf{S} + \\ + \omega H^{-1}(2\,H_x\,S_x - H_y\,S_y - H_z\,S_z) \\ + A_0\,\mathbf{I}.\mathbf{S} + \alpha(2\,I_x\,S_x - I_y\,S_y - I_z\,S_z)$$

where the indices are to be cyclically permuted for $\mathcal{H}^y$ and $\mathcal{H}^z$,

$$\Omega = \tfrac{1}{3}(g_{\parallel} + 2\,g_{\perp})\,\mu_B\,H\,, \\ \omega = \tfrac{1}{3}(g_{\parallel} - g_{\perp})\,\beta H\,, \quad A_0 = \tfrac{1}{3}(A_{\parallel} + 2\,A_{\perp})\,, \\ \alpha = \tfrac{1}{3}(A_{\parallel} - A_{\perp})$$

and H is the magnitude of the applied magnetic field.

The effect of the phonons is again represented by a statistical model for the time variation of S. The probability per unit time of a reorientation — change in value of S — is supposed to depend only on its instantaneous value and not on its past history. In addition, each distortion is supposed equally probable. S is treated as a stochastic variable, its time variations as obeying a stationary Markov process with equal probabilities for jumping to either of the two other distortions, the total transition probability for jumping out of a given distortion being $\omega_c\ s^{-1}$. By solving the resulting Chapman-Kolmogorov equation, one finds

$$P_{ii}(\tau) = \tfrac{1}{3}(1 + 2\exp - \tfrac{3}{2}\,\omega_c\,\tau) \\ P_{i\neq j}(\tau) = \tfrac{1}{3}(1 - \exp - \tfrac{3}{2}\,\omega_c\,\tau)$$

where $P_{ij}(\tau)$ is the conditional probability of S having its jth value at time τ if it had its ith value at time 0. We can now calculate such ensemble averages as

$$\overline{a_i(t)\,a_j(t+\tau)}\,.$$

The pure adiabatic case corresponds to H along a principal axis. Let

$$\mathbf{H} = H(0, 0, 1)$$

then

$$\mathcal{H} = \Omega S_z + A_0\,\mathbf{S}.\mathbf{I} + (2\,a_3 - a_1 - a_2)\,[\omega + \alpha I_z]\,S_z + \\ + \alpha(2\,a_1 - a_2 - a_3)\,S_x\,I_x + \alpha(2\,a_2 - a_3 - a_1)\,S_y\,I_y\,. \tag{4}$$

The static spectrum consists of 2 groups of 4 hyperfine structure lines at frequencies

$$\Omega_m + 2\,\omega_m \quad \text{and} \quad \Omega_m - \omega_m$$

if

$$\Omega_m = \Omega + A_0\,m_I \\ \omega_m = \omega + \alpha m_I$$

the second group corresponding to the 2 possible « perpendicular » distortions and so having twice the integrated intensity of the first. The dynamic spectrum presents a single averaged group of 4 hyperfine lines at frequencies Ω_m.

The fluctuating term $(\omega + \alpha I_z)\,S_z$ is diagonal in the eigenvectors of $\Omega S_z + A_0\,\mathbf{S}.\mathbf{I}$ and so contributes an adiabatic width of order ω_c in static limit and $(\omega + \alpha m_I)^2/\omega_c$ in the dynamic limit ; in the static limit, the two superposed « perpendicular » spectra will have one half the width of the « parallel » spectrum, since on reorienting it has an equal chance of jumping to the equivalent perpendicular distortion as to the parallel one, whereas the parallel oriented sites are obliged to jump to a perpendicular orientation. For the « averaged » spectrum, where a single group of 4 hyperfine lines with the isotropic g-value and hyperfine separation A will be seen, the widths of the hyperfine lines are asymmetric in m_I as the field from the nucleus may add or substract from the orbital electronic contribution (anisotropic g-value term ω). This, as has been several times remarked [21], is the origin of the unequal widths of the averaged spectrum for H along [100]. There is also a non-adiabatic contribution to the line width from the other fluctuating term of order $\dfrac{\alpha^2\,\omega_c}{\Omega^2 + \omega_c^2}$ which is always smaller than the adiabatic part ; by a factor $(\alpha/\Omega)^2$ in the static limit and $(\omega/\Omega)^2$ in the dynamic limit.

Using the method outlined by Kubo [18] for the adiabatic width, we find, if ν is the circular frequency of the r. f. field,

$$\chi''(\nu, \omega_c) = \\ = \text{Cte} \sum_m (\tfrac{3}{2}\,\omega_c)^2/(\Omega_m + 2\,\omega_m - \nu)^2\,(\Omega_m - \omega_m - \nu)^2 + \\ + (\tfrac{3}{2}\,\omega_c)^2\,(\Omega_m - \nu)^2\,. \tag{5}$$

In the limit $\omega_c \ll \omega$, we may write this as a sum over resonance lines of Lorentzian shape at

centre frequency (ν_0)	width ($1/T_2$)	relative integrated intensity
$\Omega_m + 2\,\omega_m$	ω_c	1
$\Omega_m - \omega_m$	$\frac{1}{2}\,\omega_c$	2

whereas for $\omega_c \gg \omega$, the lines are again Lorentzian but characterized by

Ω_m	$\dfrac{4}{3}\,\dfrac{\omega_m^2}{\omega_c}$	3 .

There is no longitudinal relaxation of $< S_z >$, for the fluctuating terms are either diagonal in S_z or off diagonal in I_z.

The pure non-adiabatic case corresponds to the magnetic field along a trigonal axis. Let

$$\mathbf{H}_0 = H_0(1, 1, 1)\,.$$

In this case we choose a set of axes (XYZ) whose Z-axis lies along (1, 1, 1), X axis along (1, − 1, 0) and

Y-axis along (1, 1, − 2). The hamiltonian may then be written

$$\mathcal{H} = \Omega S_z + A_0\, \mathbf{S}.\mathbf{I} + \\ + \sqrt{3}(\omega + \alpha I_Z)\,(a_\varepsilon\, S_X - a_\theta\, S_Y) \\ + \sqrt{3}\,\alpha S_Z(a_\varepsilon\, I_X - a_\theta\, I_Y) \\ - \tfrac{3}{2}\,\alpha(a_+\, S_+\, I_+ + a_-\, S_-\, I_-)\,, \qquad (6)$$

where

$$a_\pm = a_\theta \pm \mathrm{i}a_\varepsilon$$

$$a_\theta = \sqrt{\tfrac{1}{2}}(a_1 - a_2)\,, \quad a_\varepsilon = \sqrt{\tfrac{1}{6}}(2\,a_3 - a_1 - a_2)$$

$$\bar{a}_\theta = \bar{a}_\varepsilon = \overline{a_\varepsilon(t)\, a_\theta(t+\tau)} = 0$$

$$\overline{a_\theta(t)\, a_\theta(t+\tau)} = \overline{a_\varepsilon(t)\, a_\varepsilon(t+\tau)} = \tfrac{1}{3} \exp - \tfrac{3}{2}\,\omega_c\, |\, t - \tau\,|\,.$$

All three fluctuating terms are non-adiabatic. The fully averaged line positions are

$$\Omega_m \approx \Omega + A_0\, m_I\,.$$

One expects the non-adiabatic widths to be of order

$$\frac{(\omega + \alpha m_I)^2\, \frac{3}{2}\,\omega_c}{\Omega^2 + (\frac{3}{2}\,\omega_c)^2}$$

from the first term,

$$\frac{\alpha^2\, \omega_c}{(\frac{1}{2}\,A)^2 + (\frac{3}{2}\,\omega_c)^2}$$

from the second term and

$$\frac{\alpha^2\, \omega_c}{\Omega^2 + \omega_c^2}$$

from the third term. This last term is always smaller than the first and we shall not explicitly calculate it. A second order perturbation calculation of the evolution of the density matrix prepared by a $\pi/2$ pulse on the m_I hyperfine component gives the following frequency shifts $\Delta\omega$ and transverse decay rates : $1/T_2$:

$$\Delta\omega = \frac{\alpha^2\, A_0\, m_I}{A_0^2 + 9\,\omega_c^2} + (\omega + \alpha m_I)^2\, \frac{\Omega + A_0\, m_I}{(\Omega + A_0\, m_I)^2 + \frac{9}{4}\,\omega_c^2}$$

$$\frac{1}{T_2} = \frac{3\,\alpha^2\, \omega_c (I(I+1) - m_I^2)}{A_0^2 + (3\,\omega_c)^2} + \\ + (\omega + \alpha m_I)^2\, \frac{\frac{3}{2}\,\omega_c}{(\Omega + A_0\, m_I)^2 + (\frac{3}{2}\,\omega_c)^2}\,.$$

The conditions for this perturbation approach to be reasonably accurate are that

$$\frac{\alpha^2}{A_0^2 + (3\,\omega_c)^2} \ll 1\,, \quad \frac{(\omega + \alpha m_I)^2}{\Omega^2 + (\frac{3}{2}\,\omega_c)^2} \ll 1\,.$$

The second condition is always satisfied, for

$$\frac{\omega}{\Omega} \sim \frac{\Delta g}{g} \sim 10\ \%\,,$$

but the first is rather bad for $3\,\omega_c \lesssim A_0$, since $\alpha \approx A_0$. There is also a third order term which can be of the same order as the cross product in the second term when $\omega_c \ll A$. We discuss it below.

We shall now try to describe qualitatively the spin dynamics in the three regimes.

The spin hamiltonian for the i-distortion is $(i, j = x, y, z)$

$$\mathcal{H}^i = \sum_j \Omega_j^i\, S_j + \sum_j A_j^i\, I_j\, S_j$$

where

$$\Omega_j^i = \sqrt{\tfrac{1}{3}}(\Omega + \omega(3\,\delta_{ij} - 1))$$

$$A_j^i = A_0 + \alpha(3\,\delta_{ij} - 1)$$

$$A_0 \ll \Omega\,.$$

$\mathbf{S}$ sees an instantaneous effective field

$$\mathbf{H}_E = (\Omega_x^i + A_x^i < I_x >^i,\ \Omega_y^i + A_y^i < I_y >^i,\ \Omega_z^i + A_z^i < I_z >^i)$$

$i = x, y$ or z. It precesses around the average effective field $\overline{\mathbf{H}_E(\Omega)}$ seen on its precession time scale $1/\Omega$. The average of $< \mathbf{S} >^i$ lies along $\overline{\mathbf{H}_E(\Omega)}$, its conserved projection being M_S $(= \pm \frac{1}{2})$. The nuclear spin $\mathbf{I}$ sees an instantaneous effective field

$$\mathbf{H}_N^i = (A_x^i < S_x >^i,\ A_y^i < S_y >^i,\ A_z^i < S_z >^i) \qquad i = x, y \text{ or } z$$

and precesses about its average $\overline{\mathbf{H}_N(A)}$ on a nuclear precession time scale $1/A$, its projection m_I on this direction being conserved. Whence $< \mathbf{I} >$ to put into $\mathbf{H}_E^i$; this nuclear contribution to averaged resonance frequency $|\,\overline{\mathbf{H}_E(\Omega)}\,|$ is the observed hyperfine structure.

We can divide the behaviour into 3 regimes, depending where ω_c is placed on the A, Ω time scales.

Static regime 1 : $\omega_c \ll A,\ \Omega$

$$\overline{\mathbf{H}_E(\Omega)} = \mathbf{H}_E^i \qquad i = x, y, z$$

e. g. $\mathbf{H}_E^x(\Omega) = \sqrt{\tfrac{1}{3}}(\Omega + 2\,\omega,\ \Omega - \omega,\ \Omega - \omega)$ c. p. for y, z

$$< \mathbf{S} >^x = \sqrt{\tfrac{1}{3}}\,\Omega_I^{-1}(\Omega + 2\,\omega,\ \Omega - \omega,\ \Omega - \omega)\, M_s$$

i. e. S has a different quantization axis for each distortion

$$\overline{\mathbf{H}_N^x(A_0)} = \sqrt{\tfrac{1}{3}}\,\Omega_I^{-1}\, M_s \times \\ \times \big((A_0 + 2\,\alpha)\,(\Omega + 2\,\omega),\ (A_0 - \alpha)\,(\Omega - \omega),\ (A_0 - \alpha)\,(\Omega - \omega)\big) \quad \text{c. p. for } y, z$$

is then the average field seen by the nucleus due to the electron ; we note that $\mathbf{I}$ has a different quantization axis for each distortion.

Hence, the Zeeman frequency Ω_I is given by

$$\Omega_I^2 = \Omega^2 + 2\,\omega^2 \qquad \text{for } x, y \text{ and } z$$

and the effective hyperfine constant A_I by

$$\Omega_I^2 A_I^2 = \tfrac{1}{3}\{(A_0+2\alpha)^2(\Omega+2\omega)^2+2(A_0-\alpha)^2(\Omega-\omega)^2\} \quad \text{for } x, y \text{ or } z .$$

These are the standard static formulas (Bleaney, 1953).

Intermediate regime II : $A_0 \ll \omega_c \ll \Omega$

$$\overline{\mathbf{H}_E(\Omega)} = \mathbf{H}_E^i \qquad i = x, y \text{ or } z .$$

$< S >^i$ as for regime I — there are 3 distinct quantization axes since $\omega_c \ll \Omega$

$$\mathbf{H}_N(A) =$$

$$= \tfrac{1}{3} M_s \sum_i (A_x^i < S_x >^i, A_y^i < S_y >^i, A_z^i < S_z >^i)$$

$$= (3 A_0 \Omega + 6 \alpha\omega)(1, 1, 1) M_s/3 \Omega_I$$

there is a unique quantization axis for **I**, since $\omega_c \gg A_0$, hence

$$\Omega_{II} = \Omega_I$$

$$\Omega_I A_{II} = A_0 \Omega + 2 \alpha\omega .$$

Rapid regime III : $\omega_c \gg A_0, \Omega$

$$\overline{\mathbf{H}_E(\Omega)} = \tfrac{1}{3}\sum_i \mathbf{H}_E^i = \Omega \sqrt{\tfrac{1}{3}}(1, 1, 1)$$

there is a unique quantization axis for **S** since $\omega_c \gg \Omega$

$$< \mathbf{S} >^i = \sqrt{\tfrac{1}{3}}(1, 1, 1) M_s \qquad i = x, y \text{ or } z$$

$$\overline{\mathbf{H}_N(A)} = \tfrac{1}{3}\sum_i \sqrt{\tfrac{1}{3}}(A_x^i, A_y^i, A_z^i) M_s$$

$$= A_0 M_s \sqrt{\tfrac{1}{3}}(1, 1, 1)$$

there is again a unique quantization axis for **I**, since $\omega_c \gg A_0$ hence

$$\Omega_{III} = \Omega$$

$$A_{III} = A_0 .$$

These expressions afford us a useful check on the perturbation theory approximations in the appropriate limits. Below we develop these expressions for $\alpha/A_0 \ll 1$ and $\omega/\Omega \ll 1$ on the left and compare them with the perturbation theory frequency shifts on the right :

$$\left.\begin{aligned} \Omega_I &= \Omega + \omega\frac{\omega}{\Omega} & \Omega + \omega\frac{\omega}{\Omega} \\ A_I &= A_0 + 4A_0\frac{\omega}{\Omega} + \frac{\alpha^2}{A} & A_0 + 2A_0\frac{\omega}{\Omega} + \frac{\alpha^2}{A} \end{aligned}\right\} \quad (7.I)$$

$$\left.\begin{aligned} \Omega_{II} &= \Omega_I & \Omega_I \\ A_{II} &= A_0 + 2A_0\frac{\omega}{\Omega} & A_0 + 2A_0\frac{\omega}{\Omega} \end{aligned}\right\} \quad (7.II)$$

$$\left.\begin{aligned} \Omega_{III} &= \Omega & \Omega \\ A_{III} &= A_0 & A_0 \end{aligned}\right\} \quad (7.III)$$

The error of $2A_0\,\omega/\Omega$ in regime I arises from a third order perturbation term. The zero-order hamiltonian used was $\mathcal{H}_0 = \Omega S_z + A_0 S_z I_z$ whereas the real static hamiltonian also had a $A_0(S_x I_x + S_y I_y)$ part which should be included in the « perturbation » term. It does nothing to second order, but there are terms like

$$< \tfrac{1}{2}m \mid \alpha S_z I_- \mid \tfrac{1}{2}m+1 > < \tfrac{1}{2}m+1 \mid \omega S_+ \mid -\tfrac{1}{2}m+1 > < -\tfrac{1}{2}m+1 \mid A_0 S_- I_+ \mid \tfrac{1}{2}m >$$

which have states lying A_0 away from the starting state and so are really of second order. A detailed evaluation of these terms shows a contribution to the frequency shift of

$$\Delta\omega^{(3)} = 2 m_I \alpha \frac{\omega}{\Omega}\frac{A}{A_0^2 + (3\omega_c)^2}$$

but no contribution to the damping. This is just the missing quantity in the static $\omega_c \ll A_0$ limit, which $\to 0$ for $\omega_c \gg A_0$.

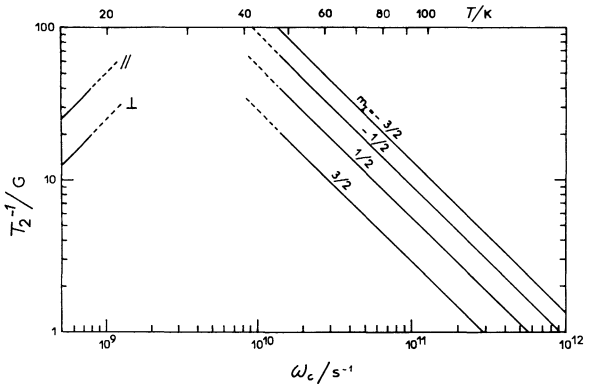

FIG. 10. — Variation of the width of the four hyperfine lines with the tunneling rate ω_c when H is along a < 100 > direction as given by eq. (5). The temperature indicated is deduced from the values of ω_c by using the T^3 law. The central part of the curves has not been plotted because linewidth is not well defined for these values of ω_c. The two curves, for low temperatures, correspond to the parallel and the perpendicular groups of lines.

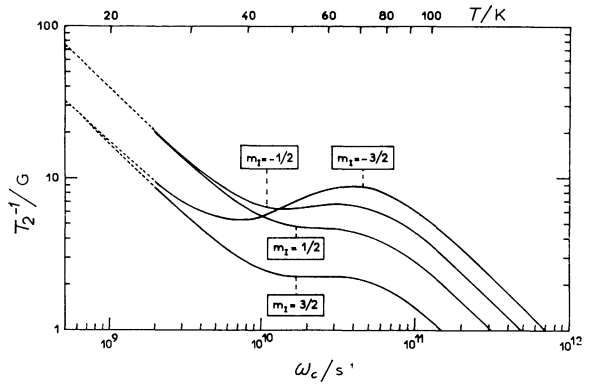

FIG. 11. — Variation of the width of the four hyperfine lines with the tunneling rate ω_c when H is along a < 111 > direction as given by eq. (5). The temperature indicated is deduced from the values of ω_c by using the T^3 law. The dotted part cannot be used in our case because the conditions of validity (6) are not fulfilled.

We have sketched the behaviour of these widths and shifts as a function of ω_c on figures 10 and 11 for the two particular orientations $< 100 >$ and $< 111 >$ of the magnetic field. Perhaps the most striking feature is the double hump in the non-adiabatic width for H along $< 111 >$ corresponding to averaging criteria first for the hyperfine structure and then for the g-value. For H along a $< 100 >$ axis, the adiabatic width shows an ill defined maximum somewhere around $\omega_c \approx \omega$ (the line is very different from Lorentzian in this region), to fall, as ω_c increases, parallel but 2 times greater than the non-adiabatic line width for $< 111 >$. At sufficiently higher temperatures, « classical » spin-lattice interaction will broaden the lines again until they finally disappear.

3.3 EFFECTS OF A TRIGONAL FIELD. — The clearest manifestation of the trigonal field is to be seen at high temperatures where the « Jahn-Teller » anisotropy is averaged out and the resonance spectrum shows axial symmetry about the (111) axis. At low temperatures, this effect is superposed on that of the frozen in tetragonal distortions, tipping the principal directions of the g and A tensor ellipsoids away from the $< 100 >$ axes and giving them a rhombic character. It is the alignment of the principal directions of g-tensors belonging to different distortions which gives rise to the nulls of the longitudinal spin relaxation rate $(1/T_1)$ in full cubic symmetry. By tilting the g-tensor ellipsoids, the trigonal field destroys this alignment so that the quantization axes for different distortions are *never* coincident.

The modifications of the g-tensor have already been discussed in II [5], but as there were some numerical errors we will rewrite the formulas. Eq. (14) of II, the Zeeman spin Hamilton in the E-spatial manifold before applying the unitary transformation S, should read :

$$\mathcal{H}_z = g_0 \mathbf{hS} - g_1 \hat{P}_0 + 4\sigma h_\tau A_2 + 2P\sigma[-2\gamma\hat{P}_1 + \beta\hat{P}_2 - \hat{P}_3] \tag{8}$$

where the operators

$$\hat{P}_0 = \{\{\mathbf{hS}\}^E U\}^{A_1} = (3h_z S_z - \underline{h}.\underline{S}) U_\theta + \sqrt{3}(h_x S_x - h_y S_y) U_\varepsilon$$

$$\hat{P}_1 = \{\mathbf{hS}\}^{T_2}_\tau = \underline{h}.\underline{S} - 3h_\tau S_\tau$$

$$\hat{P}_2 = \{\{\mathbf{hS}\}^{T_2} U\}^{T_2}_\tau = (3h_z S_z - \mathbf{hS} + 3h_\sigma S_\sigma - 3h_\rho S_\rho) U_\theta + \\ + (\sqrt{3} h_x S_x - \sqrt{3} h_y S_y + 3h_\sigma S_\rho + 3h_\rho S_\sigma) U_\varepsilon$$

$$\hat{P}_3 = \{\{\mathbf{hS}\}^{T_1} U\}^{T_2}_\tau = \sqrt{2}(h_\tau S_\rho - h_\rho S_\tau) U_\theta - \sqrt{2}(h_\sigma S_\tau - h_\tau S_\sigma) U_\varepsilon$$

will be recognized as tensor products with

$$h_\rho = \sqrt{\tfrac{1}{6}}(2h_z - h_x - h_y), \quad h_\sigma = \sqrt{\tfrac{1}{2}}(h_x - h_y), \quad h_\tau = \sqrt{\tfrac{1}{3}}(h_x + h_y + h_z),$$

and similar definitions for S_ρ, etc. ;

$$A_2 = \begin{bmatrix} & i \\ -i & \end{bmatrix}, \quad U_\theta = \begin{bmatrix} 1 & \\ & -1 \end{bmatrix} \quad \text{and} \quad U_\varepsilon = \begin{bmatrix} & 1 \\ 1 & \end{bmatrix}$$

are matrices acting on the E (spatial) subspace. The constants in the equation are given by

$$g_0 = g_s - 2P(2 + \tfrac{5}{2}P)$$

$$g_1 = 2P(1 + \tfrac{1}{2}P)$$

$$P = \lambda/\Delta, \qquad \sigma = \sqrt{\tfrac{1}{2}} < E\theta \mid V_3 \mid E\rho > /\Delta$$

λ is the spin-orbit coupling constant, V_3 the trigonal field whose axis is the [111] direction and Δ is the splitting from the $3\,d^9\ T_2$ state.

$$\gamma = 1 - R, \quad \beta = 1 - 2R, \quad R = \frac{\sqrt{2}}{4} \frac{< T_2 \tau \mid V_3 \mid T_2 \tau >}{< E\theta \mid V_3 \mid T_2 \rho >},$$

$R = -\frac{1}{2}$ for a purely quadrupolar (Y_2^0) field. The symmetry labelling is that of Griffiths [23], whose book on tensor algebra for finite groups underlies these calculations.

The equivalent effective spin hamiltonian in the E-space for the hyperfine interaction is

$$\mathcal{H}_{hfs} = A_0 \mathbf{S.I} - A_1 \hat{Q}_0 + \frac{2}{7}\mathfrak{I}\sigma\left[-2(1 + 7\gamma P)\hat{Q}_1 + (1 + 7\beta P)\hat{Q}_2 - \frac{7}{2}\kappa P \hat{Q}_3\right] \tag{9}$$

where the tensor products $\hat{Q}_i$ are defined in exactly the same way as the $\hat{P}_i$ with h replaced by $\underline{I}$. The constants

$$A_0 = \mathfrak{T}(-\kappa - 4P - P^2 + 2\kappa P^2)$$

$$A_1 = \mathfrak{T}\frac{2}{7}\left(1 + \frac{17}{2}P + P^2 + \frac{7}{8}\kappa P^2\right)$$

$$\mathfrak{T} = 2\beta\gamma_n \hbar \left\langle \frac{1}{r^3} \right\rangle$$

$$\kappa = -\frac{8\pi}{3} |\psi(0)|^2 \left\langle \frac{1}{r^3} \right\rangle^{-1}.$$

It is hoped that eq. (8) is correct to 3rd order in perturbation theory while eq. (9) is correct to 3rd order in the contact and orbital terms but is missing all the 3rd order dipolar terms (estimated to be only about 20 % of the contact + orbital 3rd order terms).

The principal values and directions of **g** and **A** tensors for the z-distortion (at low temperature) are seen to be

$$g_x = g_0 + 2C_2 g_1 + 4\sigma P(2C_2\beta - \gamma) \quad \text{along} \quad [1, -1, 0]$$

$$g_y = g_0 + 2C_2 g_1 - 4\sigma P(2C_2\beta - \gamma) \quad \text{along} \quad [1, 1, -2\psi]$$

$$g_z = g_0 - 4C_2 g_1 \quad \text{along} \quad [\psi, \psi, 1]$$

$$A_x = A_0 + 2C_2 A_1 + \frac{4}{7}\sigma\mathfrak{T}(2C_2 - 1 + 7P(2C_2\beta - \gamma)) \quad \text{along} \quad [1, -1, 0]$$

$$A_y = A_0 + 2C_2 A_1 - \frac{4}{7}\sigma\mathfrak{T}(2C_2 - 1 + 7P(2C_2\beta - \gamma)) \quad \text{along} \quad [1, 1, -2\Phi]$$

$$A_z = A_0 - 4C_2 A_1 \quad \text{along} \quad [\Phi, \Phi, 1]$$

where

$$\psi \approx -\frac{1}{3}\sigma\frac{(\gamma + C_2\beta)}{C_2} \quad \text{if} \quad P, \sigma \ll 1$$

$$\Phi \approx -\frac{1}{6}\sigma\frac{1 + C_2 + 7P(\gamma + C_2\beta)}{C_2\left(1 + \frac{17}{7}P\right)} - \sigma\frac{\kappa\mathfrak{T}C_2}{A_0 - C_2 A_1} \quad [24],$$

and C_2 is as defined by eq. (27*b*) in reference [5] and discussed at some length in reference [3] ; here it should approach its asymptotic value of $\frac{1}{2}$.

The high temperature fully averaged spectrum is described by $\frac{1}{3}$ trace of the Hamiltonian transformed to the G_x G_y G_z set of paper II, leaving only the unit matrix terms viz :

$$\mathcal{H}'_z = g_0 \mathbf{h}.\mathbf{S} - 4P\sigma\alpha(\mathbf{h}.\mathbf{S} - 3h_\tau S_\tau)$$

$$\mathcal{H}'_{hfs} = A_0 \mathbf{I}.\mathbf{S} - \frac{4}{7}\mathfrak{T}\sigma(1 + 7\gamma)(\mathbf{I}.\mathbf{S} - 3I_\tau S_\tau).$$

These averaged g and A tensors are of course axially symmetric about the trigonal axis with anisotropies

$$g'_{\|} - g'_{\perp} = 12P\sigma\gamma$$

$$A'_{\|} - A'_{\perp} = \frac{12}{7}\mathfrak{T}\sigma(1 + 7\gamma P)$$

while the « centres of gravity » are the same for the low temperature and high temperature spectra

$$g'_{\|} + 2g'_{\perp} = g_{\|} + 2g_{\perp} = 3g_0$$

$$A'_{\|} + 2A'_{\perp} = A_{\|} + 2A_{\perp} = 3A_0.$$

We remark that σ and α may be got from the ratios

$$\frac{\Delta A'}{\Delta A} = \frac{A'_{\|} - A'_{\perp}}{A_{\|} - A_{\perp}} = -\frac{\sigma(1 + 7\gamma P)}{\left(1 + \frac{17}{2}P\right)C_2}$$

$$\frac{\Delta g'}{\Delta g} = \frac{g'_{\|} - g'_{\perp}}{g_{\|} - g_{\perp}} = -\frac{\sigma\gamma}{C_2\left(1 + \frac{P}{2}\right)}.$$

The low temperature « $\perp$ » components of the tensors

are to be understood as the average of the X and Y components.

4. **Discussion.** — In this section we shall firstly compare the theoretical results obtained in section 3 with the experimental spectra, and then make some comments on the T_1 and τ measurements and the anisotropy of T_1.

4.1 COMPARISON OF THE THEORY OF THE AVERAGING WITH THE EXPERIMENTS. — As in section 2, we distinguish the two cases corresponding to the magnetic field orientations along $< 100 >$ and $< 111 >$.

4.1.1 *H along* $< 100 >$. — The effect of the tunneling on the spectrum is entirely reflected by the adiabatic formula (4) obtained with the Kubo method. Assuming that up to 40 K the T^3 law for ω_c is still valid, we have deduced the value of ω_c corresponding to the temperature at which the experimental spectra of figure 6 have been obtained and we have superposed the calculated theoretical spectrum for this value.

The general features are well accounted for :

(i) The perpendicular group of lines is seen at higher temperature than the parallel group, a consequence of the fact that every jump is effective for the latter but only one in two for the former.

(ii) In the intermediate temperature range, the « shift » of the line is very well illustrated.

(iii) For $T = 46$ K even the asymmetry of the line is reproduced.

For higher temperatures, the formula (4) alone cannot account for the experimental results. If, however, we add to the width (4/3) (ω_m^2/ω_c), corresponding to the case of strong motional narrowing, an additional contribution $1/T_1$, independent of m_1, which could arise from a classical Van Vleck mechanism, we can reproduce the spectrum considering ω_c and T_1 as adjustable parameters. In order to have a better fit, we have added eight Lorentzian lines to take into account the existence of the two copper isotopes. Figure 2 shows the fit obtained at 78 K for $\omega_c = 1.5 \times 10^{10}\ s^{-1}$ and $1/T_1 = 2.4 \times 10^7\ s^{-1}$. This value of ω_c can be compared to the value $\omega_c = 6 \times 10^{10}\ s^{-1}$ deduced from the T^3 law extrapolated to high temperature. It thus seems that the T^5 term for the reorientation rate is not effective at this temperature but even the contribution of the T^3 term is reduced. This can be understood by recalling that this law is obtained with the approximation $\theta_D \gg T$, θ_D being the Debye temperature. As θ_D for the zinc fluosilicate is relatively low, this approximation is not good and the temperature dependence is less than T^3.

We can point out that, with the help of the theory of section 3, including the influence of the trigonal field, the high temperature spectrum permits the determination of $A_\perp$ which cannot be measured at low temperature due to quadrupolar effects. Indeed, from the experimental values of $A_\parallel$, $A'_\parallel$ and $A'_\perp$, formula (10) gives $| A_\perp | = (14 \pm 2)\ 10^{-4}$ cm and $A_\parallel . A_\perp < 0$.

4.1.2 *H along* $< 111 >$. — The theory of the averaging for this orientation has been given in section 3. Figure 11 shows the variation of the linewidths as a function of the tunneling rate ω_c as given by eq. (5). The temperatures indicated on this figure are again deduced, from the law $\omega_c = BT^3$.

In our case, with the values $A_0 = 26 \times 10^{-4}\ cm^{-1}$, $\alpha = 40 \times 10^{-4}\ cm^{-1}$, the conditions (6) for the validity of this result are fulfilled only when $\omega_c \gg 3 \times 10^7\ s^{-1}$ and thus we cannot compare quantitatively the experimental width with this result for the slow regime. Nevertheless, we observe between say 4.2 K and 12 K a strong change of the hyperfine structure which corresponds to the transition from the slow regime to the intermediate regime. During this transition, the hyperfine structure constant goes from

$$A_{[111]} = \sqrt{\frac{A_\parallel^2 + 2 A_\perp^2}{3}} \quad \text{to} \quad A'_\parallel$$

(see section 3.3) while the g value remains $g_{[111]}$. We observe that, for $T = 10.1$ and 12.7 K, both type of spectra are present, as was observed for the $< 100 >$ orientation.

In the intermediate regime, which ranges from $\omega_c \sim 4 \times 10^8\ s^{-1}$ to (15 K $< T <$ 40 K) the following theoretical features are observed on the experimental spectra :

(i) At 25 K, the $m_I = \pm \frac{3}{2}$ hyperfine lines are narrower than the $m_I = \pm \frac{1}{2}$.

(ii) At 45 K, the $m_I = -\frac{3}{2}$ and $m_I = \pm \frac{1}{2}$ lines have nearly equal widths.

(iii) The $m_I = +\frac{3}{2}$ line is always narrower than the three others.

When the temperature increases again, the fast regime is obtained for which the g value becomes $g'_\parallel$ (or nearly $(g_\parallel + 2\, g_\perp)/3$). When $\omega_c \gg 8 \times 10^9\ s^{-1}$ ($T \gg 40$ K) the second term of eq. (5) is dominant and the widths are equal to $2\, \omega_m^2/3\, \omega_c$ i. e. half the value found for H along a $< 100 >$ direction. We have again tried to fit the experimental spectrum with a calculated spectrum consisting of eight Lorentzian lines having this width plus a contribution $1/T_1$ due to the classical Van Vleck mechanism. The figure 3 shows the experimental spectrum obtained at 78 K and the spectrum calculated with

$$\omega_c = 9 \times 10^9\ s^{-1} \quad \text{and} \quad 1/T_1 = 2.1 \times 10^7\ s^{-1}.$$

The values of these two adjustable parameters compare very well with those obtained with the magnetic field along a $< 100 >$ direction. The difference between the extrapolated value of ω_c using the T^3 law and the value deduced from the fitting is thus confirmed.

In conclusion, we can say that the transition from the low temperature to the high temperature spectrum, either with H along $< 100 >$ or $< 111 >$, is well explained by the theory of the averaging. We have not looked in detail at other orientations but we have observed an intermediate regime only with the field near $< 111 >$. This is also in agreement with the theory because it is only when the g values associated with each well are nearly equal that the non adiabatic terms become important.

4.2 COMMENTS ON THE RELAXATION TIME T_1 AND THE REORIENTATION TIME τ. — 4.2.1 *Temperature dependence and order of magnitude.* — A detailed calculation of the reorientation rate due to phonon assisted tunneling in the case of a Cu^{2+} ion in a cubic field with a small trigonal component has been made previously in II. We have used the results of this theory to interpret our experimental data. Neglecting the mixing between the states associated with each well induced by the spin-orbit coupling and the trigonal crystal field, the results of this theory can be summarized as follow :

Direct process :

$$\frac{1}{\tau} = 2\,A\Gamma^2\,kT\,.$$

Raman process :

$$\frac{1}{\tau} = \frac{8\,\pi^3\,\hbar A^2}{45}\left[\varepsilon^2(kT)^5 + \frac{15}{8\,\pi^2}\,\Gamma^2(kT)^3\right]$$

where

$$A = \frac{6(Bc_2)^2}{5\,\pi\hbar^4\,dv_T^5}\left[1 + \frac{2}{3}\left(\frac{v_T}{v_L}\right)^5\right];$$

d is the crystal density, v_T and v_L are the longitudinal and transverse sound velocities, B is the coupling coefficient between the center and the phonons, c_2 a parameter nearly equal to 0.5, Γ caracterizes the interwell tunneling, and ε is related to the overlap between localized states (see II for a more precise definition of these various parameters).

A word can be said on the existence of the T^3 and T^5 terms in the expression of the transition probability for a jump from one well to another. The T^3 term comes, as Pirc *et al.* [25] have shown, from the fact that there is no direct coupling between the localized states. The transition is only permitted by a mixing produced by the tunneling term Γ. One can then say that one has to go to the third order in time dependent perturbation theory. The denominator of such a term is then of the form

$$\left|(\omega_p \pm \delta)(\omega'_p \pm \delta')\right|^2$$

where ω_p and ω'_p are the frequencies of the two phonons involved, δ and δ' are the splittings between the localized states induced by random strains. As $\omega_p \sim \omega_{p'} \gg \delta, \delta'$ the denominator becomes ω_p^4 and thus, the usual T^7 law in the two phonons process is reduced to the T^3 law. The T^5 term is due to the existence of an overlap between the localized states which is responsible for a direct coupling between them. The value of this overlap is connected to the quantity ε. In that case, the denominators of the terms giving the transition probability are of the form

$$(\omega_p \pm \delta)^2 \sim \omega_p^2\,,$$

leading to the T^5 law. Of course, both ε and Γ decrease when, the warping being more and more important, the states become more and more localized. The variation of these quantities has been calculated in II.

The relaxation time T_1 is related to the reorientation time τ by :

$$\frac{1}{T_1} = \frac{1}{\tau}\left(\frac{\Delta g}{g}\right)^2\left[\lambda_x^2\,\lambda_y^2 + \lambda_y^2\,\lambda_z^2 + \lambda_z^2\,\lambda_x^2\right] \equiv \frac{1}{\tau}\cdot R\,,$$

where $\Delta g = g_{\parallel} - g_{\perp}$, $g_{\parallel} = \frac{1}{3}(g + 2\,g_{\perp})$, λ_i are the direction cosines of the magnetic field. The ratio R is a result of the non orthogonality of the spin states in different wells.

The following features of the results are in agreement with the theory :

(i) We have observed the same temperature dependence for T_1 and τ at low temperature.

(ii) The temperature dependence is T^3.

We can calculate within the model the temperatures T_c and T'_c at which the T^3 law takes over the T law and the T^5 law takes over the T^3 law :

$$kT_c = \sqrt{\frac{B}{\pi hA}}$$

$$kT'_c = \frac{\sqrt{2}}{\pi}\cdot\frac{\Gamma}{\varepsilon}\,.$$

Using the estimations given in II, we find $T'_c \sim 140$ K, a value compatible with our experiments. As we do not observe the T law, even at the lowest temperatures, we can deduce that the coupling coefficient B is stronger in fluosilicate than in double nitrate where the T law is present. If we take $T_c \sim 2$ K, we find $B > 50\,000$ cm^{-1} a value which is comparable with the value calculated in II within the D model, i. e. supposing the same stiffness for the octahedron and the environment. This result is only semi quantitative and ought to be confirmed by static stress experiments that we plan to do.

4.2.2 *Anisotropy of* T_1. — The anisotropy we have found, as that observed by Breen *et al.* on double nitrate [4] is less than the theory predicts. In particular, the T_1 for H along a $< 100 >$ axis is predicted to be infinite while the actual values are in the millisecond to microsecond range at low temperature. Such a disagreement between theoretical and experimental values of relaxation times is often observed, particularly when the theoretical time is

very long. The reasons are rarely very clear as many mechanisms can be at the origin of the faster relaxation time observed, the cross relaxation being the most cited and perhaps also the most active. We shall here consider some other possibilities.

In terms of the theory, the infinite value for T_1 when H is along $< 100 >$ axis results from the perfect orthogonality of the spin up state associated with one well with the spin down state associated with another. It is clear that anything which destroys this orthogonality will lead to a finite value for T_1. The first possibility we consider is the existence of a mosaic structure within the crystal. The magnetic field cannot then be along a $< 100 >$ direction for all the ions. For a desorientation θ, the value for T_1 is such that $\tau/T_1 = 2\ \theta^2(\Delta g/g)^2$ as compared to $\tau/T_1 = \frac{1}{3}(\Delta g/g)^2$ when H is along a $< 111 >$ axis. We have no experimental indication on the value of the r. m. s. desorientation, but orders of few degrees are frequently observed. Taking $\theta \sim 2^o$, we find $T_1 < 100 > / T_1 < 111 > \sim 5\,000$.

The second possibility we look for is the influence of the trigonal field. We have mentioned in section 3.3, that this field tilts the principal axis of the g tensors associated to each well. When H is along say [001], the quantisation axis associated with the three wells make between them the angles β_{xy}, β_{xz}, β_{yz} given by

$$\beta_{xy} = \psi(a - 1)$$

$$\beta_{yz} = \beta_{xz} = \psi\left(\frac{7}{2} - 2\,a - \frac{3}{a} + \frac{a^2}{2} + \frac{1}{a^2}\right)^{1/2}$$

where ψ is given by eq. (9) and $a = g_{\|}/g_{\perp}$. The values of the parameters σ and γ introduced in 3.3 can be estimated from the spectroscopic results using eq. (11) of section 3.3. With $\Delta g' = -0.01$, $\Delta g = 0.36$, $\Delta A' = -8.4 \times 10^{-4}\,\mathrm{cm}^{-1}$, $\Delta A = 120 \times 10^{-4}\,\mathrm{cm}^{-1}$, one gets $\sigma \sim 0.06$, $\gamma \sim 0.24$ and $\beta = 2\,\gamma - 1 = -0.52$. Thus, $\psi \sim -\dfrac{\sigma(2\,\gamma - C_2)}{3\,C_2}$ is very badly determined as $2\,\gamma \sim C_2$. From the experimental accuracy, one can only deduce that $|\psi| < 6 \times 10^{-2}$ and then $|\beta_{xy}| < 10^{-2}$, $|\beta_{xz}| = |\beta_{yz}| < 6 \times 10^{-3}$. Using the fact that

$$\frac{1}{T_1} = \frac{1}{6\,\tau}(\beta_{xy}^2 + \beta_{yz}^2 + \beta_{xz}^2),$$

we obtain $\tau/T_1 < 3 \times 10^{-5}$ for H along [001]. As this ratio is $\frac{1}{3}(\Delta g/g)^2 \sim 8.7 \times 10^{-3}$ for H along [111], we see that the trigonal field reduces the ratio $T_1 < 100 > / T_1 < 111 >$ from infinity to 300.

The anisotropy of the hyperfine tensor is, as pointed out by Ham [3], another origin for the nonorthogonality of the states associated to different wells when H is along a $< 100 >$ direction. Interwell transitions, in which electronic and nuclear spins simultaneously flip are then permitted ; coupled with the fast interwell transitions which conserve the spin orientations, they induce, in a definite well, say i, transitions like

$$|\, i, m_s = \tfrac{1}{2}, m_I, > \rightarrow |\, i, m_s = -\tfrac{1}{2}, m_I + 1 > .$$

However, as we observe the relaxation via a $\Delta m_I = 0$ line, these transitions are not active and thus cannot be responsible for the reduction of the anisotropy of T_1.

In conclusion, we see that noneof these mechanisms is strong enough to reduce the theoretical anisotropy of the relaxation time T_1 to the observed value.

Conclusion. — We have analysed in some detail, both experimentally and theoretically, the dynamical behaviour of a system showing the so called static Jahn-Teller effect. Firstly, we have related the spin lattice relaxation times T_1 to the tunneling time τ between the wells associated with distortions of the $Cu^{2+}(OH_2)_6$ octahedron and our results, which show the same temperature dependence for T_1 and τ, give additional support to the model previously proposed in II. The observed anisotropy for T_1 is however not explained by this model and the various mechanisms we have considered are not strong enough to justify our experimental observations.

Then, we have studied the « transition » from the anisotropic low temperature spectrum (the static Jahn-Teller spectrum) to the nearly isotropic high temperature spectrum. The general features of these spectra, like the magnetic field orientation dependence of the « transition temperature », the simultaneous presence of the two sorts of spectra in a definite temperature range, the strong change of the hyperfine structure when H is along a $< 111 >$ direction as well as some more subtle details like the variation of the linewidths with the temperature and the relative values of these widths for the hyperfine lines with H along $< 111 >$ are well explained by a theory based on the stochastic method and using the ideas of Anderson and Kubo. This good agreement, which confirms the validity of the tunneling model, shows that the evolution of the spectra observed with other systems equivalent to ours (see section 2.5 for references to some of these systems) probably could also be explained in detail by appropriately adapting the theory. The conclusions of Borcherts *et al.* [12], attributing the isotropic spectrum observed in Cu^{2+} : NaCl to the thermal population of an excited vibronic singlet should perhaps be reconsidered : the major argument used for this interpretation is the coexistence in a certain temperature range of the two types of spectra and we have seen this is fully compatible with the averaging. We think the theory given here could also probably be extented to systems analogous to ours because if the specific situations are different, the physics is essentially the same. The advantage of the system studied here, which permits extraction of the characteristic details, is its relative simplicity as

compared to others (see for instance the spectra of the phosphorous vacancy pairs studied by Watkins *et al.* [15]).

Acknowledgments. — The authors are happy to thank D. Breen for his collaboration during the first phase of this work. They also want to thank I. Doula of Service des Basses Températures of CEN-Grenoble for his help in lending and using a Hewlett-Packard assembly for the synthetisation of the spectra (Fig. 2 and 3) and J. C. Domais for his contribution in the relaxation time measurements.

References

[1] JAHN, H. A. and TELLER, E., *Proc. R. Soc.* (*London*) **A 161** (1937) 220.

[2] ABRAGAM, A. and PRYCE, M. H. L., *Proc. Phys. Soc.* (*London*) **A 63** (1950) 409.

[3] For a survey see HAM, F. S., in *Electron Paramagnetic Resonance*, edited by Geschwind S. (Plenum, New York) 1972.

[4] BREEN, D. P., KRUPKA, D. C. and WILLIAMS, F. I. B., *Phys. Rev.* **179** (1969) 231.

[5] WILLIAMS, F. I. B., KRUPKA, D. C. and BREEN, D. P., *Phys. Rev.* **179** (1969) 255.

[6] BLEANEY, B. and INGRAM, D. J. E., *Proc. Phys. Soc.* (*London*) **A 63** (1950) 408.

[7] WYCKOFF, R. W. G., *Crystal Structures* (Interscience Publishers, New York) **3** (1965) 797.

[8] BLEANEY, B., BOWERS, K. D. and TRENAM, R. S., *Proc. R. Soc.* (*London*) **A 228** (1955) 157.

[9] A preliminary report of these results has been given in Ampere Congress in Turku, 1972 (to be published).

[10] BERTHIER, Y., Thesis, Université Scientifique et Médicale de Grenoble I, 1966 (unpublished).

[11] LEE, K. P. and WALSH, D., *Phys. Lett.* **27A** (1968) 17.

[12] BORCHERTS, R. H., KANZAKI, H. and ABE, H., *Phys. Rev.* **B 2** (1970) 23.

[13] WILSON, R. G., HOLUJ, F. and HEDGECOCK, N. E., *Phys. Rev.* **B 1** (1970) 3609.

[14] REINBERG, A. R. and ESTLE, T. L., *Phys. Rev.* **160** (1967) 263.

[15] WATKINS, G. D. and CORBETT, J. W., *Phys. Rev.* **134** (1964) A 1359.

[16] ANDERSON, P. W., *J. Phys. Soc. Japan* **9** (1954) 316.

[17] ANDERSON, P. W. and WEISS, P. R., *Rev. Mod. Phys.* **25** (1953) 269.

[18] KUBO, R., in *Fluctuation, Relaxation and Resonance in Magnetic Systems*, edited by Ter Haar D. (Oliver and Boyd, Edinburgh and London) 1962.

[19] WINTER, J. M., in *Quantum Optics and Electronics*, Summer School des Houches 1964, edited by De Witt, Blandin and Cohen-Tannoudji (Gordon and Breach, New York) 1964.

[20] ABRAGAM, A., *The Principles of Nuclear Magnetism* (Oxford U. P., London) 1961.

[21] ORTON, J. W., AUZINS, P., GRIFFITHS, J. H. E. and WERTZ, J. E., *Proc. Phys. Soc.* (*London*) **78** (1961) 554.

[22] ABRAGAM, A. and BLEANEY, B., *Electron Paramagnetic Resonance of Transition Ions* (Clarendon Press, Oxford, England) 1970.

[23] GRIFFITH, J. S., *The Irreducible Tensor Method for Molecular Symmetry Groups* (Prentice-Hall, Englewood Cliffs, New Jersey) 1962.

[24] The second term of Φ arises from the anti-symmetric part of the A « tensor » ; such a term also exists for ψ, but is of order P compared to the symmetric contribution. For a general discussion, see ABRAGAM and BLEANEY [22], p. 651.

[25] PIRC, R., ZEKS, B. and GOSAR, P., *J. Phys. & Chem. Solids* **27** (1966) 1219.